

Patch-Token Aligned Bayesian Prompt Learning for Vision-Language Models

Xinyang Liu^{*1} Dongsheng Wang^{*1} Miaoge Li¹ Zhibin Duan¹ Yishi Xu¹ Bo Chen¹ Mingyuan Zhou²

Abstract

For downstream applications of vision-language pre-trained models, there has been significant interest in constructing effective prompts. Existing works on prompt engineering, which either require laborious manual designs or optimize the prompt tuning as a point estimation problem, may fail to describe diverse characteristics of categories and limit their applications. We introduce a Bayesian probabilistic resolution to prompt learning, where the label-specific stochastic prompts are generated hierarchically by first sampling a latent vector from an underlying distribution and then employing a lightweight generative model. Importantly, we semantically regularize prompt learning with the visual knowledge and view images and the corresponding prompts as patch and token sets under optimal transport, which pushes the prompt tokens to faithfully capture the label-specific visual concepts, instead of overfitting the training categories. Moreover, the proposed model can also be straightforwardly extended to the conditional case where the instance-conditional prompts are generated to improve the generalizability. Extensive experiments on 15 datasets show promising transferability and generalization performance of our proposed model.

1. Introduction

Large-scale vision-language pre-trained models (VLPs) have recently led to impressive results on various computer vision (CV) tasks (Wang et al., 2021; Jia et al., 2021; Cho et al., 2021; Radford et al., 2021; Li et al., 2022). Pre-trained on web-scale image-text association pairs, such VLPs have the ability to carry the semantic knowledge on which visual concepts correspond to which textual sequence and vice versa, which has been proven beneficial for visual un-

^{*}Equal contribution ¹Xidian University ²The University of Texas at Austin. Correspondence to: Bo Chen <bchen@mail.xidian.edu.cn>.

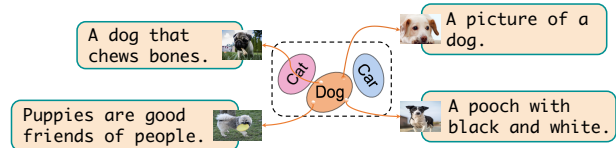


Figure 1. The core idea that multiple prompts are generated from the label-specific distributions.

derstanding (Radford et al., 2021; Mei et al., 2022; Du et al., 2022). This has motivated the rapid rise of *prompting learning* that hopes to fine-tune VLPs by formalizing the downstream tasks as language modeling problems and optimizing only the text inputs (prompts) (Radford et al., 2021; Zhou et al., 2022a;b), such as “a photo of a {class}.”, where the “{class}” token denotes the real class name. In contrast to supervised learning with discrete labels from a closed set of categories, prompt learning receives knowledge from pre-trained language models and supports open-set visual concepts, often producing better performance, especially on few/zero-shot tasks (Zhou et al., 2022a; Gu et al., 2022).

However, identifying the optimal prompts for the target label is a non-trivial task in VLPs and often requires domain knowledge and time-consuming attempts. For example, CLIP (Radford et al., 2021) ensembles 80 hand-crafted prompts to generate the corresponding label embeddings, such as “a photo of {class}.” and “a painting of a {class}.”. Rather than manually designing prompts, quite a few recent works focus on continuous prompt learning in the embedding space (Zhou et al., 2022b; Yao et al., 2021; Chen et al., 2022). Relaxing the human interpretability of prompts, they optimize the deterministic prefix tokens as learnable embedding vectors with a task-specific loss, achieving state-of-the-art results in visual classification tasks.

Though effective, some recent studies report that such models suffer from suboptimal prompt learning in terms of diversity and generalizability (Zhu et al., 2022; Ma et al., 2022; Lu et al., 2022). The diversity issue comes from the deterministic prompt assumption, where only a sentence is searched to represent a class. Intuitively, one class can be modeled by many intrinsic attributes. Thus, it is critical to learn multiple prompts that focus on different

concepts. Motivated by this, a few works introduce the uncertainty in prompt learning and attempt to generate distributed prompts (Derakhshani et al., 2022; Lu et al., 2022). However, they either require artificial prompts or focus on the uncertainty in the image domain, failing to deeply explore the knowledge in the text domain.

For the generalizability issue, unfortunately, there are no clear theoretical explanations in the community (Ma et al., 2022; Gao et al., 2021). Recent studies have introduced various techniques to enhance the transferability, including conventional anti-overfitting tricks, instance-specific prompt generation, and gradient flow (Gao et al., 2021; Zhou et al., 2022a; Ma et al., 2022; Zhu et al., 2022). Despite the improvement on few/zero-shot tasks, how to balance the base and new categories remains an open problem.

To this end, this paper proposes Bayesian prompt learning, where the label-specific stochastic prompts are generated hierarchically under the Bayesian framework. First, We introduce the uncertainty directly in the label domain and model each label with a variational distribution (Kingma & Welling) over the word embedding space. The to-be-inferred posterior contains meta-information about the corresponding category, showing advantages over point estimation in modeling uncertainty and highly structured data (Fan et al., 2020). Second, a lightweight generative network is then employed to generate the prefix embeddings according to the sampled vector from the variational distribution. Though the generative network is a deterministic mapping, the output prompts can be viewed as an implicit distribution in the embedding space due to its random inputs, which enables the proposed model to naturally handle diverse visual concepts, resulting in robust prompt learning.

Moreover, to address the over-fitting issue in prompt learning, we propose a novel semantic alignment between visual patches and textual tokens under the optimal transport (OT) framework (Villani, 2009). Specifically, we formulate the prompt-token set and image-patch set within the same category as two empirical distributions, which share similar semantics about the corresponding class, while from different modalities. Therefore, prompt learning can be viewed as the process of learning the distribution of prompt tokens to be as close to the distribution of visual patches as possible. Fortunately, the recent developments in OT provide us with an efficient tool to quantify the difference between two discrete distributions with different supports (Cuturi, 2013; Peyré et al., 2019; Zhao et al., 2021a). Importantly, the cost function in OT specifies the similarities between the prompt tokens and visual patches in the embedding space, which makes it possible to regularize the learning of tokens with visual guidance. As a result, the aligned prompts are encouraged to capture the true label-specific visual concepts, rather than over-fitting to the training set.

The main contributions of this paper are summarized as follows:

- We propose the Bayesian prompt learning that generates the label-specific stochastic prompts hierarchically, which models each label as a distribution over the embedding space, and successfully handles the diverse visual concepts.
- To avoid over-fitting to the training set, we introduce the OT distance as a regularization that guides the learning of prompts with visual knowledge by aligning the patches and tokens semantically.
- We formulate the proposed model as a variational inference problem, and a combined loss function is derived to optimize all parameters efficiently. Extensive experiments show that our models outperform the baselines.

2. Related Work

Prompt Learning in VLPs Prompt learning originates from the NLP domains with the motivation to best use the pre-trained language models (Brown et al., 2020; Shin et al., 2020; Liu et al., 2023), and it has received increasing research attention in VLPs due to its impressive results (Ge et al., 2022; Sun et al., 2022; Feng et al., 2022). For example, CLIP (Radford et al., 2021) in practice manually designs templates based on human knowledge and shows great potential in few/zero-shot tasks. Context Optimization (CoOp) (Zhou et al., 2022b) first introduces the continuous prompt into VLPs and views the prompt tokens as a set of learnable vectors that can be optimized by minimizing the cross entropy loss. Instead of learning static prompts, Conditional CoOp (CoCoOp) (Zhou et al., 2022a) learns an input-specific prompt by incorporating image features via a lightweight network and shows better generalization on unseen categories. The most related work to ours is Prompt Distribution Learning (ProDA) (Lu et al., 2022), which focuses on the output embeddings of prompts and employs a Gaussian distribution to model the latent representation by pre-defining K label-specific templates. However, ours is a novel Bayesian prompt generation method based on input embeddings, aiming to generate the label-specific stochastic prompts in a data-driven framework, rather than based on handcraft prompts.

Optimal Transport OT is originally developed to measure the distance of two probability distributions over metric spaces and has recently drawn great attention in many theoretic and application tasks due to the brilliant property of distribution matching (Arjovsky et al., 2017; Balaji et al., 2020; Zhao et al., 2021b; Tanwisuth et al., 2021). For example, Redko et al. (2019) address the target shift problem by aligning the domain distributions under the OT framework.

Enhanced transport distance (ETD) of (Li et al., 2020) introduce the attention-aware OT distance to measure the domain discrepancy. Guo et al. (2022) minimize the OT distance between the balance set and imbalance set for automatic re-weighting. The works that connect prompt learning with OT tend, however, to be very limited and still in the exploration stage. Prompt Learning with Optimal Transport (PLOT) (Chen et al., 2022) attempts to align the visual features and prompts (textual feature) by learning an adaptive transport plan (Rubner et al., 2000) to learn multiple comprehensive prompts. In contrast to PLOT, which focuses directly on distributions between two feature sets of distinct modalities, we intend to explore a more natural semantic relationship between image patches and prompt tokens by employing the OT distance to guide the learning of diverse prompts.

3. The Proposed Method

An overview of our proposed Patch-Token Aligned Bayesian Prompt learning (PBPrompt) is shown in Fig. 2. Below, we first briefly review the CoOp and OT distance, which are the base concepts used in this paper. Then, we introduce the technical details of our model, which aims to improve the diversity and generalizability of CoOp.

3.1. Reviews of CoOp and OT distance

Context Optimization (CoOp) of Zhou et al. (2022b) builds on CLIP-like VLPs and is a basic method for prompt learning. A VLP, such as CLIP often consists of an image encoder $f(x)$ and text encoder $g(t)$, each outputs a d-dimensional embedding for an image $x \in \mathbb{R}^{(3 \times H \times W)}$, and a sentence with L tokens $s = [w_1, w_2, \dots, w_L]$, where $w_l \in \mathbb{R}^e$ is the e-dimensional token embedding. To synthesize the class-specific weights for the classification task, CoOp designs the context prompt as $t_c = [p_1, p_2, \dots, p_{L-1}, e_c]$, where e_c is label embedding of class c , $p = \{p_l \in \mathbb{R}^e\}_{l=1}^{L-1}$ are L-1 learnable context vectors. Given $\{t_c\}_{c=1}^C$ and x , CoOp models the image label $p(y|x)$ as a Categorical distribution according to the similarity between the image and label feature with:

$$p(y|x) = \frac{\exp(\text{sim}(f(x), g(t^c))/\tau)}{\sum_c \exp(\text{sim}(f(x), g(t^c))/\tau)}, \quad (1)$$

where $\text{sim}(\cdot, \cdot)$ means the similarity function, e.g., the cosine similarity, and τ is the temperature parameter. Then one can optimize the prefix embeddings p via back-propagating the following loss through the frozen VLPs with a few training samples $\mathcal{D}^{\text{tr}} = \{(x_i, y_i)\}_{i=1}^{N_{\text{tr}}}$:

$$\mathcal{L}(p) = \mathbb{E}_{x_i, y_i} [-\log p(y_i | x_i, p)],$$

After learning, t_c can be used to generate the target classifier and classify test samples.

Optimal Transport Distance. Optimal transport (OT) distances have been commonly used for the comparison of distributions. Here we limit our discussion to OT in the discrete matching setting which is more related to our framework, although it applies to continuous distribution as well. Given two sets that contain N and M points respectively, the discrete distributions are formulated as:

$$\mathbf{P} = \sum_{n=1}^N \theta_n \delta_{e_n} \quad \text{and} \quad \mathbf{Q} = \sum_{m=1}^M \beta_m \delta_{l_m}, \quad (2)$$

where $\theta \in \Delta^N$ and $\beta \in \Delta^M$ are discrete probability vectors that sum to 1, and δ_e refers to a point mass located at point e in the embedding space. The OT distance between \mathbf{P} and \mathbf{Q} can be defined as:

$$d_{\mathbf{C}}(\theta, \beta) := \min_{\mathbf{T}} \langle \mathbf{T}, \mathbf{C} \rangle, \quad (3)$$

with $\mathbf{T}\mathbf{1}_M = \theta, \mathbf{T}^T\mathbf{1}_N = \beta,$

where $\langle \cdot, \cdot \rangle$ denotes the Frobenius dot-product and $\mathbf{1}_N$ is the N dimensional vector of ones. $\mathbf{C} \in \mathbb{R}_{\geq 0}^{N \times M}$ is the cost matrix of the transport, and C_{nm} denotes the transport cost between points e_n and l_m , such as the cosine distance $C_{nm} = 1 - \text{cosine}(e_n, l_m)$. $\mathbf{T} \in \mathbb{R}_{> 0}^{N \times M}$ denotes the transport plan to be learned. OT distance is then minimized over all the joint probabilities of $N \times M$ space with two marginal constraints. As computing the above OT distance has the cubic time complexity, we apply the Sinkhorn distance (Curi, 2013) that regularizes Eq. 3 with an entropic constraint:

$$d_{\mathbf{C}, \lambda}(\theta, \beta) = d_{\mathbf{C}}(\theta, \beta) - \lambda h(\mathbf{T}), \quad (4)$$

with $\mathbf{T}\mathbf{1}_M = \theta, \mathbf{T}^T\mathbf{1}_N = \beta.$

where $h(\mathbf{T})$ is the entropy of transport plan \mathbf{T} and $\lambda \geq 0$ is a hyper-parameter. With the Lagrange multiplier of the entropy constraint, Eq. 4 can be optimized within a few iterations by the Sinkhorn algorithm, which is widely used in recent discrete OT problems (Hu et al., 2021; Chen et al., 2022).

4. Patch-Token Aligned Bayesian Prompt Learning

The core idea behind the proposed PBPrompt is to learn distributed label-specific prompts under the Bayesian framework, as well as align the image patches and prompt tokens by minimizing the OT distance. Below, we introduce the details of PBPrompt, which consists of stochastic prompt generation, patch-token alignment, the training algorithm, and its extended conditional version.

Stochastic Prompts Generation One of the goals of PBPrompt is uncertainty modeling in prompts generation. For a target label, we assume there are various prompts

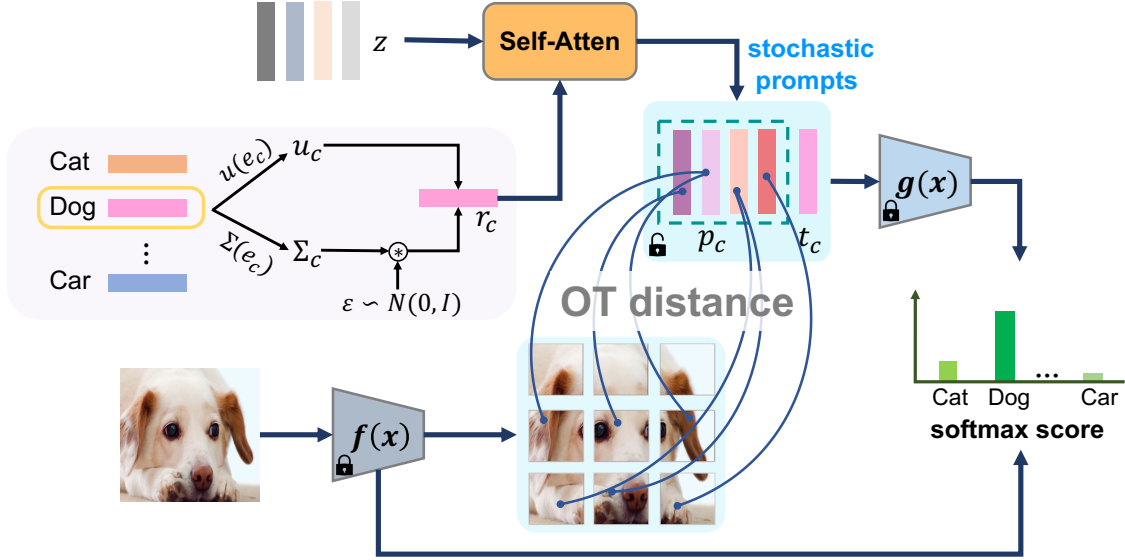


Figure 2. Overview of the proposed PBPrompt. PBPrompt generates the stochastic prompts by first sampling a label-specific vector r_c and then employing a single-layer self-attention network. OT distance is performed between the prefix tokens p_c and image patches to regularize the prompts with the vision knowledge.

that can achieve similar performance. They come from the same target class and describe its representative attributes from different aspects, *e.g.*, the object type, size, color, and so on. An intuitive approach is to model the prompts as a distribution $p(t_c)$. Unfortunately, directly learning such a distribution over a sequence of L vectors is not easy (Brown et al., 2020; Lu et al., 2022), especially under the few-shot setting. To this end, we move the uncertainty forward to its inputs and develop a hierarchical generative module to produce the stochastic prompts:

$$t_c = [\pi(p_c|r_c), e_c], \quad r_c \sim p(r_c) \quad (5)$$

where $p(r_c)$ denotes the label-specific distribution that handles the conceptual diversity of class c . $\pi(p_c|r_c)$ denotes the deterministic generative model that takes the sampled r_c as input and outputs the prefix token sequence $p_c = \{p_{c,l} \in \mathbb{R}^e\}_{l=1}^{L-1}$. Like previous works (Zhou et al., 2022b;a), the final prompt t_c is obtained by adding the label embedding e_c at the end of prefix tokens. Different from previous models that simply view t_c as the learnable embedding vectors, we generate t_c via a hierarchical path, where a stochastic vector r_c is first sampled from the label-specific distribution and the prefix sequence p_c is then generated according to r_c . Although the generative model π is a deterministic network, t_c can be viewed as an implicit distribution over r_c . In this way, multiple prompts can be generated by sampling various r_c .

Note that $\pi(p|r_c)$ can be implemented with various language models (Greff et al., 2017; Devlin et al., 2019), and we find a single-layer self-attention network works well in

most cases (Vaswani et al., 2017), empirically:

$$v_c = [r_c + \text{PE}_1, z_1 + \text{PE}_2, \dots, z_{L-1} + \text{PE}_{L-1}], \\ [\hat{r}_c, p_{c,1}, \dots, p_{c,L-1}] = \pi(p_c|r_c) := \text{Self-Atten}(v_c, v_c, v_c), \quad (6)$$

where $z = [z_1, \dots, z_{L-1}]$ is the initialized prefix embeddings, and PE is the learnable position embedding matrix that captures the sequential relations of prefix tokens. The sampled r_c can be viewed as a special label token at the beginning of the prefix sequence that contains the semantic descriptions of class c . This enables the output tokens to receive not only contextual information but also label-specific guidance.

4.1. Alignments Between Prompts and Images

Recall that a VLP often describes the target labels from both the image and text domains. The former divides the image x into N patches $\mathbf{F} = \{f_n|_{n=1}^N\} \in \mathbb{R}^{d \times N}$ and provides the local visual representations. The latter naturally has the token sequence that captures linguistic semantics discretely $\mathbf{G} = \{g_n|_{n=1}^{L-1}\} \in \mathbb{R}^{d \times L-1}$ (here, we ignore the last label token). They share similar semantics in the embedding space. To explore such multi-modality knowledge for better prompt learning, we formulate the alignment between \mathbf{F} and \mathbf{G} as an OT problem and mathematically employ two empirical distributions \mathbf{P} and \mathbf{Q} to model those two sets:

$$\mathbf{P} = \sum_{n=1}^N \theta_n \delta_{f_n}, \quad \mathbf{Q} = \sum_{l=1}^{L-1} \beta_l \delta_{g_l}.$$

We assume that patches and tokens have equal contributions to the associated image and prompt, and thus adopt

the Uniform distribution to model θ and β . With the cost matrix $C_{nm} = 1 - \text{cosine}(f_n, g_l)$, Eq. 3 provides us a novel regularization to learn label-specific prompts with vision knowledge. This enables the aligned tokens to capture meaningful visual concepts that are shared across all images within the same category, leading to more robust prompt learning and achieving a good balance between the base and new categories.

4.2. Training With Combined ELBO

Given the VLPs and labeled images \mathcal{D}^{tr} , we would like to distill the pre-trained knowledge and learn the posterior of the label-specific representation $p(r_c | \mathcal{D}^{\text{tr}})$ as well as the deterministic generative model $\pi(p_c | r_c)$. Unfortunately, the exact posterior for r_c is intractable and needs to be approximated. To this end, we define the variational distribution $q(r_c | c)$ and employ the variational inference to optimize the proposed method by minimizing the following combined Evidence Lower BOund (ELBO) (Kingma & Welling):

$$\mathcal{L} = -\mathbb{E}_{t_c = [\pi(p_c | r_c), e_c], r_c \sim q(r_c | c)} \log p(y | \mathbf{x}, t_c) - \text{D}_{\text{KL}}[q(r_c | c) || p(r_c)] + \eta d_{\text{C}, \lambda}(\theta, \beta), \quad (7)$$

where we follow previous practices (Gordon et al., 2019; Derakhshani et al., 2022) and define the variational distribution q as a Gaussian distribution conditioned on the label embedding e_c : $q(r_c | c) = \mathcal{N}(u(e_c), \Sigma(e_c))$, with u and Σ parameterized by two fully-connected layers. The first term is the expected log-likelihood defined at Eq. 1, the second term is the KL-divergence that pushes the variation posterior as close as its prior, and the last term is the OT distance that aligns the prompt tokens and image patches within the same categories. η denotes the trade-off hyperparameter that controls the regularization weights. Unlike most previous works that learn prompts only from task-specific loss (Zhou et al., 2022b; Lu et al., 2022), we optimize the proposed PBPrompt with combined ELBO that introduces the OT distance as a regularization to push the aligned tokens to focus on meaningful visual concepts rather than over-fitting to the base sets. We summarize the training algorithm in Alg. 1.

Contextual Prior $p(t^c)$ Instead of treating the prior as a fixed distribution independent of the label c , here we define the label-specific priors to further explore the semantics between labels via the label embeddings, e.g., $p(t^c) = \mathcal{N}(e_c, I)$. Compared to the fixed prior, the proposed label-specific prior introduces additional label semantics and thus achieves better prior guidance.

Conditional PBPrompt Going beyond the point estimation of prompt learning, the proposed PBPrompt generates label-specific prompts hierarchically under the Bayesian framework, giving better diversity and representation capa-

bilities. Notably, our framework can be easily extended to the conditional setting as CoCoOp (Zhou et al., 2022a) that generates adaptive prompts conditioned on the input image. Specifically, we modify Eq. 6 by updating the input v_c with the image feature \mathbf{x}_j :

$$v_{c,j} = v_c + \mathbf{W} \mathbf{x}_j, \\ \pi(p_{c,j} | r_c, \mathbf{x}_j) := \text{Self-Atten}(v_{c,j}, v_{c,j}, v_{c,j}),$$

where $\mathbf{W} \in \mathbb{R}^{e \times d}$ projects the image feature into the textual space. Compared to PBPrompt, the extended CPBPrompt can generate the label-specific instance-conditional prompts and is thus less sensitive to class shift, showing better generalization to unseen classes.

Algorithm 1 Training algorithm for our proposed PBPrompt.

Output: The trained PBPrompt, which can generate the stochastic label-specific prompts for downstream tasks.

Input: Training set $\mathcal{D} = (\mathbf{x}_j, y_j)_{j=1}^{N_{\text{tr}}}$, a VLP, class names, and hyperparameter η .

Initialize: The prefix token embeddings, the parameters in inference network $q(r_c | e_c)$ and the generative model $\pi(p_c | c)$.

for iter = 1, 2, 3, ... **do**

Sample a batch of B image-label pairs and get the image feature and patch embeddings by feeding the image into the image encoder $f(\mathbf{x})$.

Learning of PBPrompt

Generate C stochastic prompts hierarchically with Eq. 5 for all classes.

Get the token embeddings by feeding the prompts into the text encoder $g(t)$.

Compute the OT distance between patches and the corresponding prefix tokens with Eq. 3.

Compute the combined ELBO \mathcal{L} with Eq. 7 and update all learnable parameters by minimizing the \mathcal{L} with the stochastic gradient descent algorithm.

end for

5. Experiments

We follow the exact experimental setup of previous works (Zhou et al., 2022b;a) and validate the performance of PBPrompt against the recent state-of-the-art prompt learning models on widely-used benchmarks under various settings, including base-to-new generalization, cross-dataset transferability, and domain generalization.

5.1. Experimental Setup

Datasets. For the first two tasks, we rely on 11 classification datasets, *i.e.*, ImageNet (Deng et al., 2009) and Caltech101 (Fei-Fei et al., 2004) for generic object classification, OxfordPets (Parkhi et al., 2012), StanfordCars (Krause et al., 2013), Flowers102 (Nilsback & Zisserman, 2008), Food101 (Bossard et al., 2014) and FGVC Aircraft (Maji et al., 2013) for fine-grained image recognition, EuroSAT (Helber et al., 2019) for satellite image classification, UCF101 (Soomro et al., 2012) for action classification,

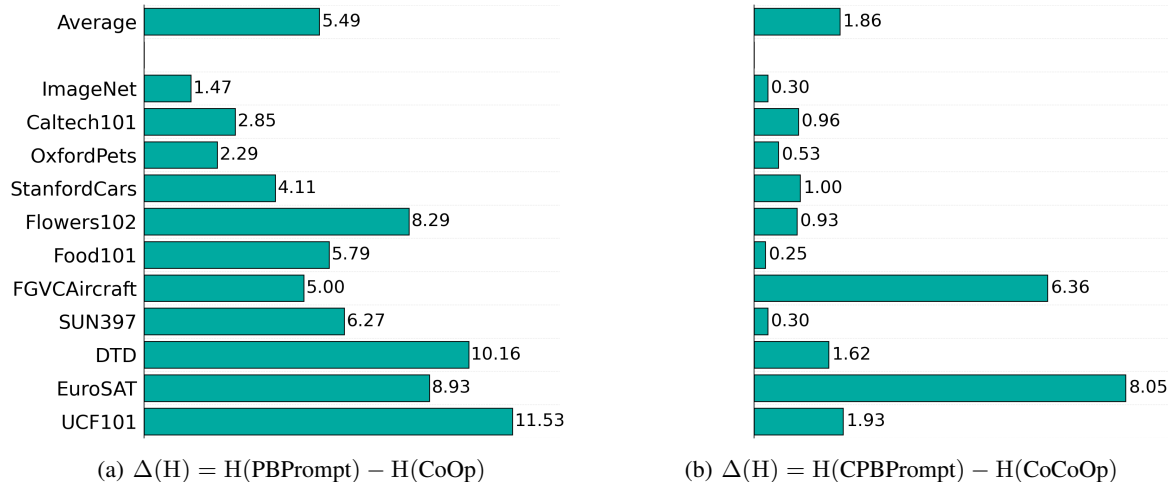


Figure 3. Absolute performance improvement of the proposed approaches over CoOp and CoCoOp in terms of harmonic mean accuracy over 11 classification datasets.

DTD (Cimpoi et al., 2014) for texture classification, and SUN397 (Xiao et al., 2010) for scene recognition. For the domain generalization task, we use ImageNet as the source domain dataset and evaluate performance on ImageNetV2 (Recht et al., 2019), ImageNet-Sketch (Wang et al., 2019), ImageNet-A (Hendrycks et al., 2021b), and ImageNet-R (Hendrycks et al., 2021a). The details of each dataset are provided in the Appendix. A. 1

Evaluation Metrics. For all problem settings, we report the average accuracy over three different random seeds. For base-to-new generalization We also report the harmonic mean $H = 2 \times (\text{base} \times \text{new}) / (\text{base} + \text{new})$, which measures the generalization trade-off between the base and new sets.

Baselines. We compare our proposed approach with following state-of-the-art (SoTa) models: zero-shot CLIP (Radford et al., 2021) with the fixed handcrafted prompt *a photo of {class}*, CoOp (Zhou et al., 2022b), CoCoOp (Zhou et al., 2022a), and the distributed prompt learning method ProDA (Lu et al., 2022). For all baselines, we adopt their results from the published papers. Moreover, To identify the impact of OT regularization on performance, we also report the results of PBPrompt without OT, *e.g.*, $\eta = 0$, and denote this variant as PBPrompt \dagger .

Implementation Details. Like previous works (Zhou et al., 2022b;a), PBPrompt adopts the vision and language encoders as a ViT-B/16 (Dosovitskiy et al., 2020) and transformer (Vaswani et al., 2017) respectively. They load the pre-trained weights of CLIP and keep frozen during training. We consistently perform prompt tuning with 16 shots and fix the prompt length as 4 for the three primary image classification tasks across all datasets. We set the trade-off

hyperparameter η as 1 and run each experiment with 10 epochs. The label embedding e_c is obtained by averaging the CLIP embedding of the class names, and we initialize the learnable prompt embedding vectors from $\mathcal{N}(0, 0.02)$. For the self-attention network in Eq. 6, we employ 8 heads for deeper interactions between prompt tokens. Other hyperparameters as well as the training pipeline are the same as Zhou et al. (Zhou et al., 2022a) in terms of definitions of few-shot tasks. (refer to Tabel. A. 2 in the appendix).

5.2. Result Analysis

Base-to-New Generalization focuses on few-shot learning task where each dataset is split into the disjoint base set and new set as in zhou et al.(Zhou et al., 2022a). Models are trained on the base set and evaluated on the new set. We report the average accuracy and harmonic mean of various models on 11 datasets at Table. 1, and also conduct comprehensive comparisons of the proposed two models and their baselines at Fig. 3. We have the following remarks about the results: *i*) Overall, our proposed models consistently outperform others in terms of New and H in most cases. Although others may have higher accuracy in few datasets, they usually cannot achieve a good balance between the base and new sets. This demonstrates that the provided Bayesian solution is in fact capable of learning more efficient prompts for downstream tasks. *ii*) Compared to non-distributed methods (CLIP, CoOp, CoCoOp), Bayesian prompt learning methods (ProDA, PBPrompt \dagger , PBPrompt, CPBPrompt) often have better performance in new and H, which is consistent with one of our motivations that learning stochastic prompts is beneficial for capturing diverse vision concepts, resulting in improved generalization. *iii*) Among the proposed PBPrompt \dagger , PBPrompt, and CPBPrompt, we find that the

Patch-Token Aligned Bayesian Prompt Learning for Vision-Language Models

Table 1. Base-to-New generalization accuracy results of various baselines on 11 datasets. We report the average value over three different seeds, and the results are performed on a 16-shot base set and then evaluated on the held-out new class. The best and the runner-up results are **highlighted** and underlined. H: the harmonic mean. PBPrompt[†] denotes the variant without OT regularization.

	Average			ImageNet			Caltech 101			Oxford Pets		
	Base	New	H	Base	New	H	Base	New	H	Base	New	H
CLIP	69.34	<u>74.22</u>	71.69	72.34	68.14	70.21	96.84	94.00	95.39	91.17	97.26	94.11
CoOp	82.66	63.22	71.65	76.14	67.88	71.77	98.00	89.81	93.72	93.67	95.29	94.47
CoCoOp	80.47	71.69	75.83	75.98	70.43	73.10	97.96	93.81	95.84	95.20	97.69	96.43
ProDA	<u>81.56</u>	72.30	76.65	75.40	70.23	72.72	98.27	93.23	95.68	95.43	97.83	96.62
PBPrompt [†]	80.74	72.51	76.40	75.73	<u>69.24</u>	72.33	97.98	94.56	96.23	95.24	96.83	96.03
PBPrompt	80.76	73.84	<u>77.14</u>	75.90	<u>70.77</u>	73.24	98.03	<u>95.17</u>	<u>96.57</u>	<u>95.53</u>	98.03	<u>96.76</u>
CPBPrompt	80.88	74.74	77.69	<u>76.02</u>	70.96	73.40	<u>98.10</u>	95.54	96.80	95.97	<u>97.98</u>	96.96
	Stanford Cars			Flowers 102			Food 101			FGVC Aircraft		
	Base	New	H	Base	New	H	Base	New	H	Base	New	H
CLIP	63.37	74.89	68.65	72.08	77.80	74.83	90.10	91.22	90.65	27.19	36.29	31.08
CoOp	78.12	60.40	68.12	<u>97.60</u>	59.67	74.06	88.33	82.26	85.18	40.44	22.30	28.74
CoCoOp	70.49	<u>73.59</u>	72.10	94.87	71.75	81.71	<u>90.70</u>	91.29	<u>90.99</u>	33.41	23.71	27.74
ProDA	74.70	71.20	<u>72.91</u>	97.70	68.68	80.66	90.30	88.57	89.43	36.90	34.13	35.46
PBPrompt [†]	72.21	70.32	71.25	94.77	70.96	81.15	90.32	90.55	90.43	34.17	32.84	33.49
PBPrompt	72.03	72.43	72.23	93.47	<u>73.60</u>	<u>82.35</u>	90.57	<u>91.37</u>	90.97	35.47	32.17	33.74
CPBPrompt	73.13	73.07	73.10	95.63	72.76	82.64	90.87	91.62	91.24	33.83	<u>34.37</u>	<u>34.10</u>
	SUN 397			DTD			EuroSAT			UCF 101		
	Base	New	H	Base	New	H	Base	New	H	Base	New	H
CLIP	69.36	75.35	72.23	53.24	59.90	56.37	56.48	64.05	60.02	70.53	77.50	73.85
CoOp	80.60	65.89	72.50	<u>79.44</u>	41.18	54.24	92.19	54.74	68.69	<u>84.69</u>	56.05	67.45
CoCoOp	<u>79.74</u>	76.86	<u>78.27</u>	77.01	56.00	64.85	87.49	60.04	71.21	82.33	73.45	77.64
ProDA	78.67	76.93	77.79	80.67	56.48	66.44	83.90	66.00	73.88	85.23	72.97	78.04
PBPrompt [†]	79.25	76.44	77.81	76.32	54.73	63.75	<u>89.46</u>	67.13	76.70	82.69	74.06	78.13
PBPrompt	79.27	<u>77.00</u>	78.11	77.13	55.27	64.40	86.03	<u>69.87</u>	<u>77.62</u>	82.67	76.60	<u>78.98</u>
CPBPrompt	79.47	77.70	78.57	78.13	<u>57.84</u>	66.47	85.90	73.56	79.26	82.63	<u>76.73</u>	79.57

Table 2. Cross-dataset transfer learning accuracy results of various baselines on source and target datasets. We first train the models on source dataset and then test it on 10 distinct target datasets. We here focus on the comparisons of the proposed models with the base CoOp and CoCoOp. Δ : The improvements of the proposed model compared to its baseline model.

Method	Source			Target									
	ImageNet	Caltech101	OxfordPets	StanfordCars	Flowers102	Food101	FGVCAircraft	SUN397	DTD	EuroSAT	UCF101	Average	
CoOp	71.51	93.70	89.14	65.41	68.71	85.30	18.47	64.15	41.92	46.39	66.55	63.81	
PBPrompt	70.90	94.43	90.62	64.81	70.40	86.13	23.95	67.41	45.62	46.20	67.47	65.70	
Δ	-0.61	+0.73	+1.48	-0.60	+1.69	+0.83	+5.48	+3.26	+3.70	-0.19	+0.92	+1.29	
CoCoOp	71.02	94.43	90.14	65.32	71.88	86.06	22.94	67.36	45.73	45.37	68.21	65.74	
CPBPrompt	70.94	94.92	90.83	65.34	72.37	86.41	24.58	67.75	45.23	45.10	68.78	66.13	
Δ	-0.08	+0.49	+0.69	+0.02	+0.49	+0.35	+2.09	+0.39	-0.50	-0.27	+0.57	+0.40	

OT regularization always has a positive improvement. We contribute this to the semantic alignments between textual tokens and visual patches, which provides a theory tool to learn prompts with vision knowledge guidance under the OT framework. Moreover, CPBPrompt is superior to PBPrompt

by generating label-specific instance-conditional prompts. This coincides with the previous empirical findings (Zhou et al., 2022a) that the image features enhance the generalization.

Table 3. Cross-domain generalization accuracy results of various baselines. The models are first trained on source domain and evaluated on 4 target domains. This experiment aims to specify the sensitivity of the models to domain shift. Δ : The improvements of the proposed model compared to its baseline model.

Method	Learnable	Source		Target		
		ImageNet	ImageNetV2	ImageNet-Sketch	ImageNet-A	ImageNet-R
CLIP	✗	66.73	60.83	46.15	47.77	73.96
CoOp	✓	71.51	64.20	47.99	49.71	75.21
PBPrompt	✓	70.90	64.40	49.10	51.00	76.40
CoCoOp	✓	71.02	64.07	48.75	50.63	76.18
CPBPrompt	✓	70.97	64.54	49.47	51.39	76.92

Cross-Dataset Transfer Learning measures the transfer performance from different sources, where we train our model on ImageNet (source dataset) and then test it on 10 distinct target datasets. As shown at Table. 2, compared to CoOp, PBPrompt has an improvement on 8 out of 10 target domains, and achieves 2.0% average improvement cross all source and target domains, demonstrating that the proposed Bayesian prompt learning has the potential to transfer beyond a single dataset. Similar performance enhancement can also be found in the conditional setting due to the novel label-specific instance-conditional strategy. Moreover, we also find that both PBPrompt and CPBPrompt exhibits large gaps on fine-grained datasets (FGCVAircraft, OxfordPets, and Flowers102), suggesting the capacity to handle the discriminative features of each category.

Domain Generalization concerns about the robustness of the distribution shift, where we assess the proposed models on ImageNetV2, ImageNet-Sketch, ImageNet-A, and ImageNet-R after training it on the source dataset (ImageNet). We report the results at Table. 3 and find that the proposed models perform the best accuracy on all target domains over other baselines, expect the case in the source domain where ours have a slight drop in performance. This demonstrates that the learned stochastic prompts are less sensitive to distribution shift and thus show promising domain generalization performance. We attribute this to the Bayesian prompt learning and OT alignment. The former handles the diverse vision concepts, resulting in robust prompt learning, and the latter pushes the aligned prompts tokens to focus on meaningful patches, rather than overfitting to the source sets.

Ablation Studies on Prior Choice. We introduce the contextual prior in Sec. 4.2 that considers the label semantics for better prior guidance. To ablate its effectiveness, we replace the label-specific prior with the non-informative prior $p(t_c) = \mathcal{N}(0, I)$ and report their comparison results with the same seed on four datasets, varying in domains, scale, and class numbers at Table. 4. We find that the proposed label-specific prior almost gives the positive improvement

Table 4. Ablation results of different prior choices.

Dataset		$N(0, I)$	$N(e_c, I)$	Δ
Caltech101	Base	98.07	98.00	-0.70
	New	93.47	94.73	+1.26
	H	95.71	96.34	+0.63
OxfordPets	Base	95.20	95.60	+0.40
	New	96.98	97.80	-0.78
	H	96.08	96.69	+0.61
Flowers102	Base	94.67	95.85	+1.18
	New	68.73	72.34	+3.61
	H	79.64	82.45	+2.81
DTD	Base	77.60	78.13	+0.53
	New	55.87	57.60	+1.73
	H	64.97	66.31	+1.34

on both base and new sets. This demonstrates the effectiveness of our way of incorporating label semantics into prior modeling.

6. Conclusion

In this paper, we propose Patch-Token aligned Bayesian prompt learning (PBPrompt) for pre-trained vision-language models. PBPrompt is a Bayesian prompt tuning method, where the label-specific stochastic prompts are generated hierarchically under the variational inference framework that consists of a stochastic sampling network and a deterministic generative model. Moreover, we also introduce an OT regularization that aligns the prompt tokens with the image patches under the optimal transport theory. PBPrompt is optimized by the derived combined ELBO via the stochastic gradient algorithm. Due to the flexibility of the proposed framework, PBPrompt can be easily extended to the Conditional PBPrompt that allows the label-specific instance-conditional prompts generation. Extensive experiments on 15 datasets at various tasks are conducted to evaluate the efficiency of our models. We hope PBPrompt will provide a simple tool for prompt tuning and inspire future works.

References

- Arjovsky, M., Chintala, S., and Bottou, L. Wasserstein generative adversarial networks. In *International conference on machine learning*, pp. 214–223. PMLR, 2017.
- Balaji, Y., Chellappa, R., and Feizi, S. Robust optimal transport with applications in generative modeling and domain adaptation. *Advances in Neural Information Processing Systems*, 33:12934–12944, 2020.
- Bossard, L., Guillaumin, M., and Van Gool, L. Food-101—mining discriminative components with random forests. In *Computer Vision—ECCV 2014: 13th European Conference, Zurich, Switzerland, September 6–12, 2014, Proceedings, Part VI 13*, pp. 446–461. Springer, 2014.
- Brown, T., Mann, B., Ryder, N., Subbiah, M., Kaplan, J. D., Dhariwal, P., Neelakantan, A., Shyam, P., Sastry, G., Askell, A., et al. Language models are few-shot learners. *Advances in neural information processing systems*, 33:1877–1901, 2020.
- Chen, G., Yao, W., Song, X., Li, X., Rao, Y., and Zhang, K. Prompt learning with optimal transport for vision-language models. *arXiv preprint arXiv:2210.01253*, 2022.
- Cho, J., Lei, J., Tan, H., and Bansal, M. Unifying vision-and-language tasks via text generation. In *International Conference on Machine Learning*, pp. 1931–1942. PMLR, 2021.
- Cimpoi, M., Maji, S., Kokkinos, I., Mohamed, S., and Vedaldi, A. Describing textures in the wild. In *Proceedings of the IEEE conference on computer vision and pattern recognition*, pp. 3606–3613, 2014.
- Cuturi, M. Sinkhorn distances: Lightspeed computation of optimal transport. *Advances in neural information processing systems*, 26, 2013.
- Deng, J., Dong, W., Socher, R., Li, L.-J., Li, K., and Fei-Fei, L. Imagenet: A large-scale hierarchical image database. In *2009 IEEE conference on computer vision and pattern recognition*, pp. 248–255. Ieee, 2009.
- Derakhshani, M. M., Sanchez, E., Bulat, A., da Costa, V. G. T., Snoek, C. G., Tzimiropoulos, G., and Martinez, B. Variational prompt tuning improves generalization of vision-language models. *arXiv preprint arXiv:2210.02390*, 2022.
- Devlin, J., Chang, M., Lee, K., and Toutanova, K. BERT: pre-training of deep bidirectional transformers for language understanding. In *Proceedings of the 2019 Conference of the North American Chapter of the Association for Computational Linguistics: Human Language Technologies, NAACL-HLT 2019, Minneapolis, MN, USA, June 2–7, 2019, Volume 1 (Long and Short Papers)*, pp. 4171–4186, 2019.
- Dosovitskiy, A., Beyer, L., Kolesnikov, A., Weissenborn, D., Zhai, X., Unterthiner, T., Dehghani, M., Minderer, M., Heigold, G., Gelly, S., et al. An image is worth 16x16 words: Transformers for image recognition at scale. *arXiv preprint arXiv:2010.11929*, 2020.
- Du, Y., Wei, F., Zhang, Z., Shi, M., Gao, Y., and Li, G. Learning to prompt for open-vocabulary object detection with vision-language model. In *Proceedings of the IEEE/CVF Conference on Computer Vision and Pattern Recognition*, pp. 14084–14093, 2022.
- Fan, X., Zhang, S., Chen, B., and Zhou, M. Bayesian attention modules. *Advances in Neural Information Processing Systems*, 33:16362–16376, 2020.
- Fei-Fei, L., Fergus, R., and Perona, P. Learning generative visual models from few training examples: An incremental bayesian approach tested on 101 object categories. In *2004 conference on computer vision and pattern recognition workshop*, pp. 178–178. IEEE, 2004.
- Feng, C., Zhong, Y., Jie, Z., Chu, X., Ren, H., Wei, X., Xie, W., and Ma, L. Promptdet: Towards open-vocabulary detection using uncurated images. In *European Conference on Computer Vision*, pp. 701–717. Springer, 2022.
- Gao, P., Geng, S., Zhang, R., Ma, T., Fang, R., Zhang, Y., Li, H., and Qiao, Y. Clip-adapter: Better vision-language models with feature adapters. *arXiv preprint arXiv:2110.04544*, 2021.
- Ge, C., Huang, R., Xie, M., Lai, Z., Song, S., Li, S., and Huang, G. Domain adaptation via prompt learning. *arXiv preprint arXiv:2202.06687*, 2022.
- Gordon, J., Bronskill, J., Bauer, M., Nowozin, S., and Turner, R. Meta-learning probabilistic inference for prediction. In *International Conference on Learning Representations*, 2019.
- Greff, K., Srivastava, R. K., Koutník, J., Steunebrink, B. R., and Schmidhuber, J. LSTM: A search space odyssey. *IEEE Trans. Neural Networks Learn. Syst.*, 28(10):2222–2232, 2017.
- Gu, Y., Han, X., Liu, Z., and Huang, M. PPT: pre-trained prompt tuning for few-shot learning. In *Proceedings of the 60th Annual Meeting of the Association for Computational Linguistics, ACL 2022*, pp. 8410–8423, 2022.
- Guo, D., Li, Z., Zheng, M., Zhao, H., Zhou, M., and Zha, H. Learning to re-weight examples with optimal transport for imbalanced classification. *Advances in Neural Information Processing Systems*, 34, 2022.

- Helber, P., Bischke, B., Dengel, A., and Borth, D. Eurosat: A novel dataset and deep learning benchmark for land use and land cover classification. *IEEE Journal of Selected Topics in Applied Earth Observations and Remote Sensing*, 12(7):2217–2226, 2019.
- Hendrycks, D., Basart, S., Mu, N., Kadavath, S., Wang, F., Dorundo, E., Desai, R., Zhu, T., Parajuli, S., Guo, M., et al. The many faces of robustness: A critical analysis of out-of-distribution generalization. In *Proceedings of the IEEE/CVF International Conference on Computer Vision*, pp. 8340–8349, 2021a.
- Hendrycks, D., Zhao, K., Basart, S., Steinhardt, J., and Song, D. Natural adversarial examples. In *Proceedings of the IEEE/CVF Conference on Computer Vision and Pattern Recognition*, pp. 15262–15271, 2021b.
- Hu, Y., Gripon, V., and Pateux, S. Leveraging the feature distribution in transfer-based few-shot learning. In *Artificial Neural Networks and Machine Learning - ICANN 2021 - 30th International Conference on Artificial Neural Networks, Bratislava, Slovakia, September 14-17, 2021, Proceedings, Part II*, 2021.
- Jia, C., Yang, Y., Xia, Y., Chen, Y.-T., Parekh, Z., Pham, H., Le, Q., Sung, Y.-H., Li, Z., and Duerig, T. Scaling up visual and vision-language representation learning with noisy text supervision. In *International Conference on Machine Learning*, pp. 4904–4916. PMLR, 2021.
- Kingma, D. P. and Welling, M. Auto-encoding variational bayes. In *2nd International Conference on Learning Representations, ICLR 2014*.
- Krause, J., Stark, M., Deng, J., and Fei-Fei, L. 3d object representations for fine-grained categorization. In *Proceedings of the IEEE international conference on computer vision workshops*, pp. 554–561, 2013.
- Li, J., Li, D., Xiong, C., and Hoi, S. Blip: Bootstrapping language-image pre-training for unified vision-language understanding and generation. *arXiv preprint arXiv:2201.12086*, 2022.
- Li, M., Zhai, Y.-M., Luo, Y.-W., Ge, P.-F., and Ren, C.-X. Enhanced transport distance for unsupervised domain adaptation. In *Proceedings of the IEEE/CVF conference on computer vision and pattern recognition*, pp. 13936–13944, 2020.
- Liu, P., Yuan, W., Fu, J., Jiang, Z., Hayashi, H., and Neubig, G. Pre-train, prompt, and predict: A systematic survey of prompting methods in natural language processing. *ACM Computing Surveys*, 55(9):1–35, 2023.
- Lu, Y., Liu, J., Zhang, Y., Liu, Y., and Tian, X. Prompt distribution learning. In *Proceedings of the IEEE/CVF Conference on Computer Vision and Pattern Recognition*, pp. 5206–5215, 2022.
- Ma, C., Liu, Y., Deng, J., Xie, L., Dong, W., and Xu, C. Understanding and mitigating overfitting in prompt tuning for vision-language models. *arXiv preprint arXiv:2211.02219*, 2022.
- Maji, S., Rahtu, E., Kannala, J., Blaschko, M., and Vedaldi, A. Fine-grained visual classification of aircraft. *arXiv preprint arXiv:1306.5151*, 2013.
- Mei, T., Corso, J. J., Kim, G., Luo, J., Shen, C., and Zhang, H. Guest editorial introduction to the special section on video and language. *IEEE Transactions on Circuits and Systems for Video Technology*, 32(1):1–4, 2022.
- Nilsback, M.-E. and Zisserman, A. Automated flower classification over a large number of classes. In *2008 Sixth Indian Conference on Computer Vision, Graphics & Image Processing*, pp. 722–729. IEEE, 2008.
- Parkhi, O. M., Vedaldi, A., Zisserman, A., and Jawahar, C. Cats and dogs. In *2012 IEEE conference on computer vision and pattern recognition*, pp. 3498–3505. IEEE, 2012.
- Peyré, G., Cuturi, M., et al. Computational optimal transport: With applications to data science. *Foundations and Trends® in Machine Learning*, 11(5-6):355–607, 2019.
- Radford, A., Kim, J. W., Hallacy, C., Ramesh, A., Goh, G., Agarwal, S., Sastry, G., Askell, A., Mishkin, P., Clark, J., et al. Learning transferable visual models from natural language supervision. In *International Conference on Machine Learning*, pp. 8748–8763. PMLR, 2021.
- Recht, B., Roelofs, R., Schmidt, L., and Shankar, V. Do imagenet classifiers generalize to imagenet? In *International Conference on Machine Learning*, pp. 5389–5400. PMLR, 2019.
- Redko, I., Courty, N., Flamary, R., and Tuia, D. Optimal transport for multi-source domain adaptation under target shift. In *The 22nd International Conference on Artificial Intelligence and Statistics*, pp. 849–858. PMLR, 2019.
- Rubner, Y., Tomasi, C., and Guibas, L. J. The earth mover’s distance as a metric for image retrieval. *International journal of computer vision*, 40(2):99–121, 2000.
- Shin, T., Razeghi, Y., IV, R. L. L., Wallace, E., and Singh, S. Autoprompt: Eliciting knowledge from language models with automatically generated prompts. In *Proceedings of the 2020 Conference on Empirical Methods in Natural Language Processing, EMNLP 2020, Online, November 16-20, 2020*, 2020.

- Soomro, K., Zamir, A. R., and Shah, M. Ucf101: A dataset of 101 human actions classes from videos in the wild. *arXiv preprint arXiv:1212.0402*, 2012.
- Sun, X., Hu, P., and Saenko, K. Dualcoop: Fast adaptation to multi-label recognition with limited annotations. *arXiv preprint arXiv:2206.09541*, 2022.
- Tanwisuth, K., Fan, X., Zheng, H., Zhang, S., Zhang, H., Chen, B., and Zhou, M. A prototype-oriented framework for unsupervised domain adaptation. *Advances in Neural Information Processing Systems*, 34:17194–17208, 2021.
- Vaswani, A., Shazeer, N., Parmar, N., Uszkoreit, J., Jones, L., Gomez, A. N., Kaiser, Ł., and Polosukhin, I. Attention is all you need. *Advances in neural information processing systems*, 30, 2017.
- Villani, C. *Optimal transport: old and new*, volume 338. Springer, 2009.
- Wang, H., Ge, S., Lipton, Z., and Xing, E. P. Learning robust global representations by penalizing local predictive power. *Advances in Neural Information Processing Systems*, 32, 2019.
- Wang, Z., Yu, J., Yu, A. W., Dai, Z., Tsvetkov, Y., and Cao, Y. Simvlm: Simple visual language model pretraining with weak supervision. *arXiv preprint arXiv:2108.10904*, 2021.
- Xiao, J., Hays, J., Ehinger, K. A., Oliva, A., and Torralba, A. Sun database: Large-scale scene recognition from abbey to zoo. In *2010 IEEE computer society conference on computer vision and pattern recognition*, pp. 3485–3492. IEEE, 2010.
- Yao, Y., Zhang, A., Zhang, Z., Liu, Z., Chua, T.-S., and Sun, M. Cpt: Colorful prompt tuning for pre-trained vision-language models. *arXiv preprint arXiv:2109.11797*, 2021.
- Zhao, H., Phung, D., Huynh, V., Le, T., and Buntine, W. L. Neural topic model via optimal transport. In *9th International Conference on Learning Representations, ICLR 2021, Virtual Event, Austria, May 3-7, 2021*, 2021a.
- Zhao, W., Rao, Y., Wang, Z., Lu, J., and Zhou, J. Towards interpretable deep metric learning with structural matching. In *Proceedings of the IEEE/CVF International Conference on Computer Vision*, pp. 9887–9896, 2021b.
- Zhou, K., Yang, J., Loy, C. C., and Liu, Z. Conditional prompt learning for vision-language models. In *Proceedings of the IEEE/CVF Conference on Computer Vision and Pattern Recognition*, pp. 16816–16825, 2022a.
- Zhou, K., Yang, J., Loy, C. C., and Liu, Z. Learning to prompt for vision-language models. *International Journal of Computer Vision*, 130(9):2337–2348, 2022b.
- Zhu, B., Niu, Y., Han, Y., Wu, Y., and Zhang, H. Prompt-aligned gradient for prompt tuning. *arXiv preprint arXiv:2205.14865*, 2022.

Appendix of “Patch-Token Aligned Bayesian Prompt Learning for Vision-Language Models”

A. Data statistics and Hyperparameter setting

Our experiments are conducted on 15 widely-used vision datasets. *E.g.*, ImageNet (Deng et al., 2009) and Caltech101 (Fei-Fei et al., 2004) for generic object classification, OxfordPets (Parkhi et al., 2012), StanfordCars (Krause et al., 2013), Flowers102 (Nilsback & Zisserman, 2008), Food101 (Bossard et al., 2014) and FGVCAircraft (Maji et al., 2013) for fine-grained image recognition, EuroSAT (Helber et al., 2019) for satellite image classification, UCF101 (Soomro et al., 2012) for action classification, DTD (Cimpoi et al., 2014) for texture classification, and SUN397 (Xiao et al., 2010) for scene recognition. For the domain generalization task, we use ImageNet as the source domain dataset and evaluate performance on ImageNetV2 (Recht et al., 2019), ImageNet-Sketch (Wang et al., 2019), ImageNet-A (Hendrycks et al., 2021b), and ImageNet-R (Hendrycks et al., 2021a). We summarize data statistics at Table. A. 1

We set the training hyper-parameters as well as the training pipeline are the same as Zhou et al. (Zhou et al., 2022a) in terms of definitions of few-shot tasks. We list those settings at Table. A. 2.

Table A. 1. Statistics of the datasets.

Dataset	Classes	Train	Val	Test
ImageNet	1000	1.28M	N/A	50,000
Caltech101	100	4,128	1,649	2,465
OxfordPets	37	2,944	736	3,669
StanfordCars	196	6,509	1,635	8,041
Flowers102	102	4,093	1,633	2,463
Food101	101	50,500	20,200	30,300
FDVCAircraft	100	3,334	3,333	3,333
SUN397	397	15,880	3,970	19,850
DTD	47	2,820	1,128	1,692
EuroSAT	10	13,500	5,400	8,100
UCF101	101	7,639	1,808	3,783
ImageNetV2	1000	N/A	N/A	10,000
ImageNet-Sketch	1000	N/A	N/A	50,889
ImageNet-A	200	N/A	N/A	7,500
ImageNet-R	200	N/A	N/A	30,000

Table A. 2. All results in the main paper were generated using shared hyperparameters.

Hyperparameters	Values
Batch Size	1
Input Size	224×224
Input Interpolation	"Bicubic"
Input Pixel Mean	[0.48145466, 0.4578275, 0.40821073]
Input Pixel STD	[0.26862954, 0.26130258, 0.27577711]
Transforms	["random resized crop", "random filp", "normalize"]
Optimizer	SGD
Learning Rate	$2e-3$
LR Scheduler	"cosine"
Warmup Epoch	1
Warmup Type	"constant"
Warmup LR	$1e-5$
Backbone	ViT-B/16
Prompt Length	4
Prompt Initialization	""
Precision	"fp16"
Number of shots	16

Dataset	Methods	1 shot	2 shots	4 shots	8 shots	16 shots
Caltech101	CoOp					
	PLOT	87.9	89.4	91.8	93.0	93.5
	PBPrompt					
DTD	CoOp					
	PLOT	52.0	55.9	58.4	65.7	70.0
	PBPrompt					
EuroSAT	CoOp					
	PLOT	60.2	68.3	73.5	79.9	83.5
	PBPrompt					
FGVCAircraft	CoOp					
	PLOT					
	PBPrompt					
Flowers102	CoOp					
	PLOT	70.4	84.5	88.5	80.7	
	PBPrompt					
FOOD101	CoOp					
	PLOT	69.3	72.7	75.2	76.7	
	PBPrompt					
ImageNet	CoOp					
	PLOT					
	PBPrompt					
OxfordPets	CoOp					
	PLOT	82.9	85.3	86.0	87.4	88.0
	PBPrompt					
StanfordCars	CoOp					
	PLOT	-	50.9	54.0		
	PBPrompt					
SUN397	CoOp					
	PLOT					
	PBPrompt					
UCF101	CoOp					
	PLOT	49.5	53.1	60.9	67.3	70.9
	PBPrompt					
Average	CoOp					
	PLOT					
	PBPrompt					

Table A. 3. The few-shot results of various methods on 11 datasets. We report mean value over 3 different seeds.